



## Pixel-based and object-oriented approaches in segregating cocoa from forest in the Juabeso-Bia landscape of Ghana



George Ashiagbor <sup>a,\*</sup>, Eric K. Forkuo <sup>b</sup>, Winston A. Asante <sup>a</sup>, Emmanuel Acheampong <sup>a</sup>, Jonathan A. Quaye-Ballard <sup>b</sup>, Prince Boamah <sup>c</sup>, Yakubu Mohammed <sup>c</sup>, Ernest Foli <sup>d</sup>

<sup>a</sup> Faculty of Renewable Natural Resources (FRNR), Kwame Nkrumah University of Science and Technology (KNUST), PMB, Kumasi, Ghana

<sup>b</sup> Department of Geomatic Engineering, Kwame Nkrumah University of Science and Technology (KNUST), PMB, Kumasi, Ghana

<sup>c</sup> Resource Management Support Centre (RMSC), Forestry Commission (FC), Ghana

<sup>d</sup> CSIR-Forestry Research Institute of Ghana (CSIR-FORIG), University PO Box UP63, Kumasi, Ghana

### ARTICLE INFO

#### Keywords:

Sentinel-1  
Sentinel-2  
Cocoa  
Cocoa deforestation  
Land cover  
REDD+  
Ghana  
Land use

### ABSTRACT

A wall-to-wall Earth Observation (EO) data is required, as recommended by the Intergovernmental Panel on Climate Change, private sector organizations and major development partners, to allow for the implementation of forest monitoring commitments, and also to monitor commodity-led deforestation. However, a major limitation associated with the use of optical EO data in the High Forest Zone of Ghana is the presence of persistent cloud cover and the spectral limitations of segregating agroforestry cocoa (AFC) from open canopy forest (OCF) cover. The aim of the study was to investigate the synergistic use of Sentinel-1 (S1) and Sentinel-2 (S2) EO data to produce a land use/land cover map which shows AFC and OCF as different land cover classes. It was hypothesized that, a hybrid method of spectral, radar and image objects will accurately segregate the different cocoa systems from forest and other land use classes. The research was conducted in the Juaboso-Bia REDD+ Hotspot Intervention Area in the cocoa-forest mosaic landscape within the High Forest Zone of Ghana. The S1 and S2 datasets were freely acquired for the periods January to March 2018. The S1 datasets were pre-processed from backscatter intensity values to the VV and VH bands. The S2 datasets were corrected for atmospheric effects, and cloud pixels were masked and filled using a temporal gap-filling method. Six vegetation indices (VIs) were extracted, and the Multiresolution Segmentation algorithm was used to derive image objects (IOs). The S2 bands, the six VIs, the S1 VV + VH data, and the IOs were stacked into 3 different multi-layer image dataset denoted with D (i.e. D1 = S2 + VIs; D2 = S2 + VIs + S1; and D3 = S2+VIs + S1+IOs). The three datasets were classified using Random Forest and 1228 training points. Overall accuracy (OA) and kappa ( $\kappa$ ) were calculated for the classification outcome using 615 independent validation points. McNemar's test ( $\chi^2$ ) was used to assess the statistically significant difference between D1, D2 and D3. The results of the study show that, D3 significantly improved the overall classification output (OA = 89.76%,  $\kappa$  = 0.877) compared to D1 (OA = 79.02%,  $\kappa$  = 0.748;  $\chi^2$  = 5.56, p-value = 0.018) and D2 (OA = 80.49%,  $\kappa$  = 0.765;  $\chi^2$  = 5.50, p-value = 0.019). Combining spectral pixels with image objects increases overall classification accuracy and specifically, the accuracy of isolating AFC from OCF. This research is significant because it will provide an improved decision support to government-led monitoring and the private sector's commitment to halt cocoa-driven deforestation. Furthermore, and most importantly, the map shows agroforestry cocoa separated from monoculture cocoa, which provides a tremendous boost to monitoring landscape-level improvements associated with the promotion and adoption of agroforestry in cocoa landscapes, as a climate-smart practice and also for monitoring various off-reserve landscape forest restoration activities.

### 1. Introduction

Over the last five decades, world cocoa production has doubled

through the extension into forest areas, resulting in the disappearance of about 15 Million ha of global forest cover (Somarriba and Lopez-Sampson, 2018). In Sub-Saharan Africa, specifically Ghana and

\* Corresponding author. Faculty of Renewable Natural Resources (FRNR), Kwame Nkrumah University of Science and Technology(KNUST), Ghana.  
E-mail addresses: [gashiagbor.canr@knust.edu.gh](mailto:gashiagbor.canr@knust.edu.gh), [tettehgeorge@gmail.com](mailto:tettehgeorge@gmail.com) (G. Ashiagbor).

Côte D'Ivoire, cocoa production is estimated to be responsible for the historical deforestation between 1988 and 2007 in most forest landscapes in the two countries (WCF, 2019; Hoare et al., 2018). Further analysis indicates that Ghana's rainforest has been converted to cocoa at a rate of 6.1% per annum between 2000 and 2011, with the few remaining reserved areas threatened (Fountain and Huetz-Adams, 2018). Given the current global demand for cocoa products (e.g. chocolate), the rate of forest loss is expected to increase in Ghana, Côte D'Ivoire and Nigeria (Fountain and Huetz-Adams, 2018; Higonnet et al., 2017; IDH, 2018). This implies that critical interventions are needed to deal with deforestation emanating from cocoa production.

In response to these threats, global and local led interventions have been put in place to strengthen forest governance and reduce deforestation. In Ghana, the European Union-led Forest Law Enforcement, Governance and Trade Voluntary Partnership Agreement (FLEGT VPA); the Reducing Emissions from Deforestation and Forest Degradation (REDD+); and more recently the Cocoa and Forests Initiative (CFI), are recognized as important intervention strategies by industry players, development partners and government to address the challenges of deforestation associated with cocoa production (Gibbs et al., 2007; IDH, 2018; Rakatama et al., 2017). These programs and strategies (i.e. REDD+, FLEGT VPA and CFI) demonstrate the Government of Ghana's commitments towards improving sustainable landscapes and interventions to monitor deforestation, with a primary focus on the High Forest Zone (HFZ), which includes the cocoa-forest mosaic landscape of Ghana (Forestry Commission, 2016; Indufor, 2015). The HFZ covers 8.2 million hectares i.e 34% of Ghana's total land mass, which consists of forests ranging from wet evergreen to dry semi-deciduous, with rich indigenous flora. It is the region with the highest precipitation, with rainfall reaching an average of 2300 mm in the wettest parts (Odoom and Varmola, 1998). Thus, forest monitoring at the landscape level constitutes an integral part of climate-smart and sustainable landscape initiatives around agro-commodities in the HFZ. To allow for the effective implementation of these forest monitoring commitments, where historical patterns of disturbance is needed to account for emissions arising from forest degradation, and also to monitor deforestation in the cocoa-forest mosaic landscape, a wall-to-wall Earth Observation (EO) data is required as recommended by the Intergovernmental Panel on Climate Change (Mitchell et al., 2017) and the CFI (IDH, 2018; Kroeger et al., 2017).

However, until now, mainly optical EO data (i.e Landsat) have been used for forest monitoring in Ghana and the establishment of Ghana's Forest Reference Level (FRL). Unfortunately, some limitations have been associated with the use of optical Landsat data for land use and land cover (LULC) mapping. These limitations present a great challenge with the implementation of REDD+ and CFI initiatives within the cocoa forest mosaic landscape. First, the cocoa forest mosaic landscape of Ghana is consistently under persistent cloud cover because of the West African monsoon climate (Xiong et al., 2017). A search through the archives of available noncommercial satellite scenes (i.e OLI Landsat 8 and Sentinel 2) for the HFZ of Ghana reveals persistent cloud cover.

Also, the HFZ of Ghana is made of an interacting mosaic of forest of different canopy and shades (classified as closed canopy and open canopy forest), cocoa, croplands and human settlement areas. The closed canopy forest constitutes primary and secondary woody vegetation stands of 1m minimum mapping unit with more than 60% crown canopy and with 5 m height, mainly found within the forest reservation areas (National REDD + Secretariat, Forest Commission, 2017). The open canopy forest represents degraded forests resulting mainly from logging activities, usually with crown cover between 15% and 60%. Some cocoa species require forest canopy to offer shade and protection from too much light and damage caused by wind creating an agroforestry system (Aneani and Padi, 2016; ICI, 2011). They grow well and in harmony with the surrounding primary/secondary forest, thriving under the shade canopy of taller, older trees (ICI, 2011). The agroforestry cocoa system represent a wide range of biodiversity, including fruit trees,

shrubs and other plants, generating at least three levels of canopy storage, one below that of cocoa and, more importantly, one or two above with different levels of shades (Ruf, 2011; Blaser et al., 2018). Other higher-yielding full-sun monoculture varieties are also cultivated in the landscape replacing the agroforestry varieties (Ruf, 2011; Blaser et al., 2018). The monoculture cocoa system often has only one level of canopy storage with minimum or no natural or planted trees within (Ruf, 2011).

The complex and heterogeneous nature of the HFZ, with the interacting mosaic of closed canopy forest, open canopy forest, agroforestry cocoa systems and monoculture cocoa presents a great challenge to mapping the landscape. This relates to limitations associated with isolating agroforestry cocoa systems from open canopy and closed canopy forest systems (Carodenuto, 2019; Numbisi et al., 2019). This is because of the spectral similarities between agroforestry cocoa systems and open canopy forest due to similarities in canopy structure (Benefoh, 2018; Numbisi et al., 2019). In most available LULC products for Ghana, cocoa and other croplands are grouped as agricultural lands (e.g Hackman et al., 2017), which presents limited benefits to efforts to identify and address cocoa driven deforestation concerns. In other cases, the agroforestry cocoa areas are classified as forest lands with very low classification accuracy (Indufor, 2015; Mahmood, 2017). For example, the Forestry Commission of Ghana completed the Forest Preservation Program which produced a LULC map for the country (Pasco Corporation, 2013), but this map failed to accurately segregate cocoa from forests. The key limitation identified was land use misclassification in relation to agroforestry cocoa being represented as open canopy forest cover, similar to other open canopy forest classes within the Forest Reserves, hence a reported increase in forest cover.

Benefoh et al. (2018) and Numbisi et al. (2019) present the only attempt in literature to isolate cocoa systems from forest and other land cover classes. Benefoh et al. (2018) used Landsat 8 optical dataset to isolate the different cocoa systems from forest cover and other land use types in the Krokosua Hills Forest Reserve catchment of Ghana. A major challenge is the use of optical Landsat 8 images which is limited due to persistent cloud cover. Numbisi et al. (2019) explored the combine use of RapidEye optical data and C-band Sentinel-1 SAR dataset to isolate agroforestry cocoa from forest cover in the Bakoa landscape of Cameroon. The RapidEye sensor is a full end-to-end commercial Earth Observation system and therefore does not provide a cost-effective and sustainable means of mapping the landscapes in resource limited developing countries. Other LULC mapping efforts of cocoa landscape exist in literature in cocoa producing countries (e.g. Akinyemi, 2013; Barima et al., 2016; Mertens and Lambin, 2000). However the focus was not on the substantive issue of isolating the different cocoa systems from forest and other landcover classes.

The cocoa landscape of Ghana constitutes a major intervention area to achieve national climate change commitments under the Ghana REDD+ strategy, Nationally Determined Contributions, as well as interventions to drive cocoa sustainability. Thus, current limitations to accurately map cocoa systems from forest and other land cover present a critical setback to land use planning decision support tools and national forest and agro-commodity monitoring interventions. This has implications for the accurate estimation and representation of cocoa and forest land use change and transitions. This difficulty further extends to current efforts to accurately map the forest restoration interventions in the cocoa-forest mosaic landscape, and the determination of improvements associated with current efforts to step up the practice of cocoa agroforestry through tree incorporation in cocoa farms. On the other hand, once there are challenges in differentiating cocoa agroforestry from open and closed canopy forests, current efforts to monitor cocoa deforestation or landscape restoration through agroforestry tree incorporation in cocoa systems will be limited, with its consequent implications for possibilities of misrepresentation of the various cocoa land uses. Thus, an accurate estimation of cocoa driven deforestation as well as landscape restoration efforts is increasingly being demanded by

industry players in order to drive climate-smart landscape certification and other cocoa landscape sustainability programs.

EO based Synthetic Aperture Radar (SAR) instruments have the advantage of capturing cloud-free datasets for forest monitoring. However, pixels in SAR represents the coherent addition of scatterers from a corresponding resolution cell which interfere, either constructively or destructively, depending on the phase of the scatterers (Yu et al., 2018; Choi and Jeong, 2019). As such, the resulting images exhibit a 'salt-and-pepper' effect known as speckles, even for homogeneous regions, that makes it difficult for visual interpretation. These inherent speckles increase measurement uncertainties and hence reduce classification accuracies (Choi and Jeong, 2019; Joshi et al., 2016; Maghsoudi et al., 2012). To overcome these limitations associated with using optical and SAR EO data for improved segregation of the cocoa systems from forest in the HFZ of Ghana, the combined use of SAR and optical appears to be promising and beneficial (Joshi et al., 2016; Lu and Weng, 2007).

The European Space Agency's Sentinel-1 C-band SAR Level-1 Single Look Complex data acquired in the Interferometric Wide swath mode (5 days temporal resolution and  $2.7 \times 22$  m to  $3.5 \times 22$  m spatial resolution) and Sentinel-2 optical data (5 days temporal resolution and 10 m spatial resolution) are freely available under an open license and provides the possibility for improved and sustainable mapping of the HFZ of Ghana (ESA, 2015, 2012; Ghasseian, 2016; Mercier et al., 2019). The high temporal resolution of Sentinel-2 provides opportunity for temporal compositing of time series data to generate a new cloud free image data for a given time epoch for the wall-to-wall mapping of the landscape (Lopes et al., 2020; Joshi et al., 2016). The Sentinel-1 and Sentinel-2 datasets provide complementary information, hence land cover classification tasks can take advantage of both data types leading generally to increase mapping accuracy (Clerici et al., 2017; Joshi et al., 2016). This is because, optical datasets provide information based on chemical composition of features while SAR microwave data backscatter radiance gives information about structural properties such as surface roughness and object density of features. The combined use of Sentinel-1 and Sentinel-2 data to address data gaps as a result of cloud cover and to improve classification accuracy is well documented in literature (Ban et al., 2017; Clerici et al., 2017; Gómez, 2017; Joshi et al., 2016; Kaplan and Avdan, 2018; Lopes et al., 2020; Tavares et al., 2019).

However, the land use classes identified in the cocoa-forest landscape e.g. the agroforestry cocoa systems, the open canopy forest and the closed canopy forest are defined based on the morphology of the classes i.e. based on the number of trees per hectare, canopy closure and level of strata (Asante et al., 2017). Secondly, the basic unit of landscapes are class patches and not pixels. Class patches are relatively distinct and vary in size, internal homogeneity, and discreteness (Blaschke and Strobl, 2001). This implies the mapping of, for example, agroforestry cocoa systems from satellite images is not a variable of spectral properties of the images only, but also a variable of the spatial pattern and pixel size of the satellite data to be used in the mapping (Blaschke and Strobl, 2001). The spatial pattern characterises the geometry, the arrangement and spatial context of the individual class patches within the landscape. For example, Ghana's adopted definition of cocoa agroforestry systems i.e. 18 emergent trees per hectare, implies that agroforestry cocoa systems occurs in different canopy closure (depending on tree species), and in different patch shapes and sizes across the entire landscape, defining the morphology of the patch. The pixel size on the other hand defines smallest spatial elements or class patches that can be distinguished in the landscape. Hence, the number of pixels that must aggregate to represent a class patch in the landscape is dependent on the spatial resolution of the satellite image. The highly heterogeneous nature of Ghana's cocoa-forest mosaic landscape implies high spectral variations within a given land cover patch/class when a high resolution EO data e.g. Sentinel-2 is used. It is therefore practical to incorporate image objects into the classification process because they describe more the characteristics of the landscape based on shape and homogeneity of neighboring pixels.

Image objects are distinct, mutually disjoint or discrete regions that are more homogeneous within themselves created by aggregating image pixels of defined characteristics through the process of image segmentation (Drăguț et al., 2010; Liu and Xia, 2010). They divide and characterize landscapes into meaningful objects (such as forest and lakes) taking into consideration spatial and spectral properties which give a better approximation of the real size and shape of land cover types (Basayigit and Ersan, 2015). Image objects incorporate spatial information into the classification process and they represent the true spatial pattern rather than pixels (Blaschke and Strobl, 2001; Wang et al., 2004). Combining spectral and backscatter pixels and image objects implies harnessing the spectral and textural capabilities of a satellite dataset and spatial patterns of the landscape and incorporating into the classification process. The combined use of image objects (object-based) and spectral satellite bands (pixel-based) classification approaches have been used in recent times to improve on overall classification accuracy (Chen et al., 2018; El-shehaby and Taha, 2018; Li et al., 2013; Salah, 2014; Salehi et al., 2013, 2011; Shackelford and Davis, 2003; Wang et al., 2004; Xie et al., 2008).

The aim of the study was to investigate the synergistic use of Sentinel-1 (S1) and Sentinel-2 (S2) datasets to produce a LULC map for the cocoa-forest mosaic landscape, which clearly isolates monoculture cocoa and agroforestry cocoa from forest and other land cover classes by means of the Random Forest (RF) Machine Learning classifier. Specifically, this study seeks to compare the sole use of spectral bands (S2 dataset) to spectral and backscatter bands (S2+S1) and the combined use of spectral, backscatter and image objects (S2+S1+image objects). The research hypothesized that a hybrid method of spectral, radar and image objects will accurately segregate the different cocoa systems (i.e. agroforestry cocoa and monoculture cocoa) and other land use classes (Salah, 2014; Salehi et al., 2013). The study was motivated by the current demand by policy makers and major stakeholders in the forestry and cocoa sectors to have a sustainable, cost-effective and accurate approach to producing a LULC map of Ghana's cocoa-forest mosaic landscape that clearly shows the different cocoa systems (AF cocoa and mono cocoa) isolated from forest (open and closed canopy forest) and other landcover classes (cropland, and other tree crops).

## 2. Methodology

### 2.1. Study area

The research was conducted in the Juaboso-Bia REDD+ hotspot intervention area in Ghana's cocoa-forest mosaic landscape within the HFZ of Ghana. The REDD+ hotspot intervention area lies within latitudes  $6^{\circ}15'$  and  $7^{\circ}$  N and longitudes  $2^{\circ}30'$  and  $3^{\circ}15'$  W (Fig. 1). The study area falls within the moist evergreen and semi-deciduous forest ecological zones. The landscape is highly undulating with elevation ranging between 133 and 627 m above mean sea level. The annual rainfall pattern is bimodal and ranges between 1250 and 1750 mm. Cocoa is the major land-use system, which occupies most of the undulating terrain and it is recognized as one of the key drivers of deforestation in the landscape (Hoare et al., 2018; Somarriba and Lopez-Sampson, 2018). Cocoa plantations exist in a range of structural complexities and specifically, in the study area, they are classified as full sun cocoa (area of monoculture cocoa) and shaded cocoa (agroforestry cocoa - cocoa farms with various degrees of shade trees) with at least two levels of strata. In a relatively small area, a cocoa system may range from full sun cocoa to a relatively closed canopy cover, then to more open canopy cocoa. Aside cocoa farms, secondary forest growth, other tree crops such as citrus, rubber and oil palm plantations also occur in different patchiness and various extents of open grasslands and croplands. Table 1 provides the definition/full description of the land-use systems used in this study. Within the study polygon is the Bia North forest reserve, the Muro forest reserve, the Sui River forest reserve, the Krokosua Hills forest reserve and the Bia National Park and Biosphere

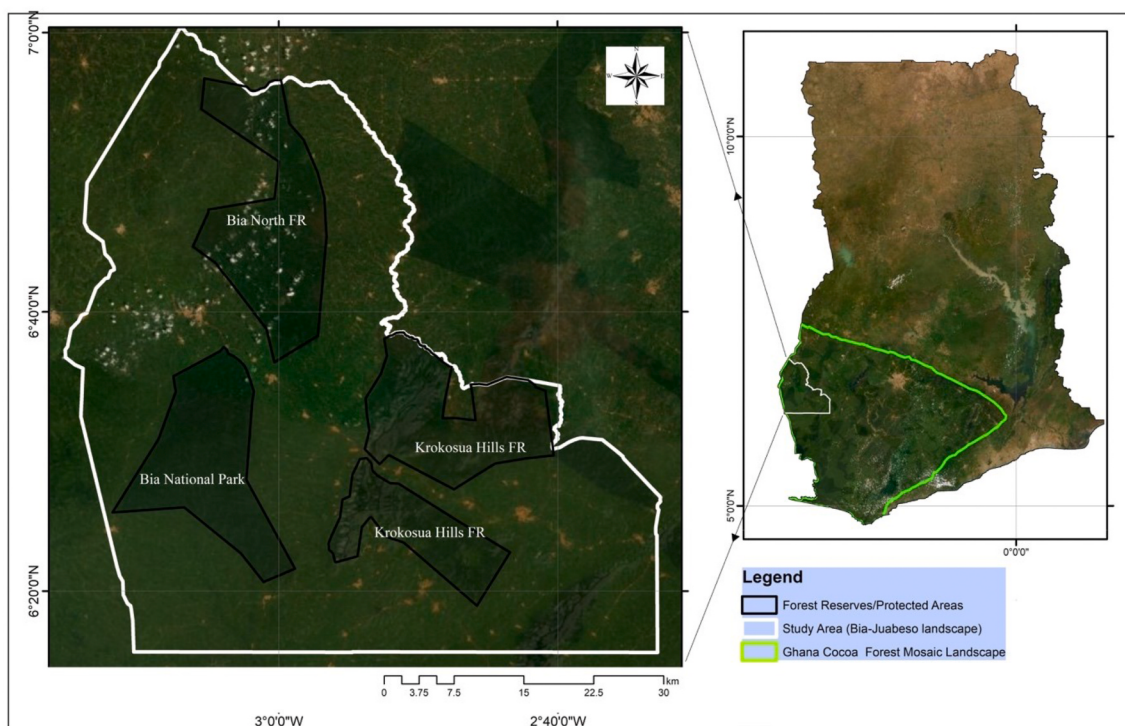


**Fig. 1.** Map of Ghana showing the Juabeso-Bia landscape in the cocoa-forest mosaic landscape (Image source: Esri, DigitalGlobe, GeoEye, Earthstar Geographics, CNES/Airbus DS, USDA, USGS, AeroGRID, IGN, and the GIS User Community).

**Table 1**  
Definitions of LULC classes used in the mapping.

LULC Class	Description
1 Closed canopy forest (CCF)	The closed canopy forest constitutes primary and secondary woody vegetation stands of 1m minimum mapping unit with more than 60% crown canopy and with 5 m height. The CCF class is mainly found within the forest reserves and protected areas
2 Open canopy forest (OCF)	The open canopy forest class represents degraded forests as resulting mainly from logging activities, usually with crown cover between 15% and 60%. The area also covers riverine vegetation usually outside the reserve and protected area.
3 Full sun cocoa/ Monoculture Cocoa (MCC)	Full sun cocoa represents monoculture cocoa farms with few or no natural or planted trees within.
4 Agroforestry cocoa (AFC)	The Agroforestry cocoa also referred to as the shaded cocoa system represents cocoa farms with natural or planted trees incorporated and creates a relatively closed canopy system with double strata. The upper canopy non-trees forming the upper strata and the cocoa canopy forming the second strata.
5 Croplands/Shrublands	These include food crops, grasslands/fallow areas and shrub vegetation.
6 Other tree crops	These are established citrus, oil palm ( <i>Elaeis guineensis</i> ) and rubber ( <i>Hevea brasiliensis</i> ) plantations within the landscape.
7 Built-up/bare soil	These include human-settlement areas, bare lands, mined areas, etc.

area. Within the forest reserves and the national park areas are the closed canopy forest covers.

## 2.2. Data acquisition

A Level-1 Single Look Complex (SLC) Sentinel-1A C-band (5.405

GHz) SAR data acquired for the periods January to March 2018 in the Interferometric Wide (IW swath) mode was used. This had a dual-polarization capability (VV + VH). Also, Level L1C Sentinel-2 datasets (Orthorectified and corrected to TOA reflectance) of the same season were obtained for the study. The Sentinel-2 datasets were freely acquired from the European Space Agency (ESA) through Sentinels Scientific Data Hub. Fieldwork was conducted to collect Global Positioning System (GPS) datasets of the different LULC systems identified in the study landscape (Table 1). Reference data were obtained through field survey using handheld GPS. GPS coordinates were collected following approximately the proportion area covered by each identified LULC class and also ensuring good spatial distribution of reference points in the study landscape. Stratified random sampling technique was used for the GPS field survey. The survey team ensured a minimum distance of 30 m (3 pixels) between sample points and also coordinates were taken at minimum 10 m distance away from the edge of the specific land cover class to compensate for GPS errors. Overall, 1838 points were collected, 308 for the agroforestry cocoa class, 230 croplands, 210 points in the built-up areas, 220 in monoculture cocoa farms, 320 in the closed canopy forest, 340 in the open canopy forest areas, and 210 points in other tree crops. The samples were randomly divided into 1228 (70%) for training and 615 (30%) for accuracy assessment.

## 2.3. Sentinel data pre-processing and variables extraction

### 2.3.1. Data processing

The Sentinel-1 data was pre-processed sequentially from backscatter intensity values to sigma naught using the Sentinel Application Platform (SNAP), an open-source software. The Sentinel-1 SAR processing chain in the SNAP software was used as a guide (<http://step.esa.int/main/tooboxes/snap/>). The image was first radiometrically calibrated to Gamma naught backscatter coefficient to relate pixel values directly to radar backscatter of the reflecting surface based on the metadata of the products (Balzter et al., 2015; Onojeghuo et al., 2018). Prior, the raw Sentinel 1 dataset was corrected for thermal noise removal and the orbit

**Table 2**

Description of Vegetation Indices (VIs) and texture measures used to retrieve biophysical information from the different cocoa systems and forest land cover.

Indices	Definition	Reference
1. Normalized Difference Vegetation Index (NDVI)	$NDVI = \frac{NIR - Red}{NIR + Red}$	Birth and McVey (1968); Pearson et al., 1972
2. Red-edge Chlorophyll Index (Red Edge CI)	$CI_{red-edge} = \left( \frac{Rededge\ 3}{Rededge\ 1} \right) - 1$	Zhang et al. (2018)
3. Plant Senescence Reflectance Index (PSRI)	$PSRI = \frac{Red - Blue}{Rededge\ 2}$	Zhang et al. (2018)
4. Green Normalized Difference Vegetation Index (GNDVI)	$GNDVI = \frac{NIR - Green}{NIR + Green}$	Barati et al. (2011); Clerici et al. (2017); Frampton et al. (2013)
5. Sentinel-2 Red-Edge Position Index (S2REP)	$S2REP = 705 + 35 \left[ \frac{\left( \frac{NIR + Red}{2} \right) - Rededge1}{Rededge\ 2 - Rededge\ 1} \right]$	Clerici et al. (2017); Frampton et al. (2013)
6. Inverted Red-Edge Chlorophyll Index (IRECI)	$IRECI = NIR - Red / (Rededge\ 1 / Rededge\ 2)$	Frampton et al. (2013)

file was applied. The orbit file are auxiliary files that contain information about the position of the satellite during image acquisition and helps in better geocoding of the SAR dataset. In this study, the latest orbit file was auto-downloaded by SNAP and applied for the geocoding of the SAR images. Speckles in the SAR image were removed using the Enhanced Lee polarimetric speckle filter (Chatziantoniou et al., 2017; Plank et al., 2017; Van Beijma et al., 2014). This is because the Enhanced Lee filter suppresses speckle noise and preserves edges, thus preserving the structure of the image (Liu, 2016; Plank et al., 2017). The Range-Doppler terrain orthorectification in SNAP was used to correct for geometric distortions due to the side-looking geometry of the SAR image (Onojeghuo et al., 2018). The images were terrain corrected using the SRTM 1 Sec DEM data, and resampled to a spatial resolution of 10 m using bilinear interpolation and re-projected to the UTM system Zone 30 North, WGS 84 (Bayanudin and Jatmiko, 2016; Cutler et al., 2012; Onojeghuo et al., 2018).

The Level 1C Sentinel-2 images were ortho-rectified, clouds detected, masked and filled using temporal gap-filling method, and corrected for atmospheric and radiometric effects using the SNAP/Sentinel-2 toolbox. First, the level 1C Sentinel-2 images were converted to level 2A and all image bands resampled to 10 m resolution using the Sen2Cor processor (<https://step.esa.int/main/third-party-plugins-2/sen2cor/>). Sentinel-2 cloud detection, masking and temporal gap-filling was performed using the image processing chain available in the Sen2Three processor in SNAP (<http://step.esa.int/main/third-party-plugins-2/sen2three/>). Sen2Three is a level 3 processor for the temporal gap-filling of Sentinel-2 level 2a images. It takes time series of level 2a images and generates a synthetic output image by replacing step by step all invalid pixels (i.e. clouds, dark features or terrain shadows, cloud shadows and thin cirrus) with the collocated valid pixels (clear sky pixels) of scenes in the time series. Six different Satellite-derived Vegetation Indices (VIs) were explored to retrieve biophysical information from the different cocoa systems and forest land cover (See Table 2). Satellite-derived VIs parameters are sensitive to photosynthetically active radiation and they provide one of the best possible means to obtain the biophysical parameters of vegetation (Benefoh et al., 2018; Frampton et al., 2013; Zhang et al., 2018). VIs can characterize different leaf and canopy attributes and have the ability to sense changes in different forest types (Barati et al., 2011; Zarco-Tejada et al., 2018). Some studies have demonstrated the effectiveness of incorporating VIs in image classification to discriminate different vegetation types (Benefoh et al., 2018; Clerici et al., 2017). Sentinel-2 provides reflectance values around the red edge at a 20 m spatial resolution, which provides the opportunity for the retrieval of biophysical parameters of vegetation

such as chlorophyll content per unit leaf area (Ch), Leaf Area Index (LAI) and leaf water content (Delegido et al., 2011; Frampton et al., 2013). Although a certain degree of redundancy is introduced by adding vegetation indices to the spectral bands, vegetation in heterogeneous environmental conditions, as in the study area, can be better detected using a set of different spectral indices (Benefoh et al., 2018; Clerici et al., 2017).

### 2.3.2. Image objects extraction using the multiresolution segmentation algorithm

Due to the high heterogeneity of the landscape and the high spectral variability within the LULC classes, a characteristic of the study, image objects were extracted and incorporated into the classification process. Image object represents the true spatial pattern rather than a uniform pixel and provides meaningful means of incorporating spatial information into the image classification procedure (Clerici et al., 2017; Wang et al., 2004). In this research, the Multiresolution Segmentation (MRS) algorithm in eCognition was used to derive image objects (El-shehaby and Taha, 2018; Salehi et al., 2013). The 10m spatial resolution Sentinel-2 level 2a image was used as input for the segmentation in eCognition. All the eight seven (blue, green, red, red-edge 1, 2, 3, and NIR) were assigned equal weights of one. Different parameters for scale, shape and compactness was experimented through a supervised iterative process until the scale of 10, shape 0.01 and compactness 0.8 provided a close representation of the highly heterogeneous landscape (See Fig. 2).

### 2.4. Image layers preparation and random forest classification

The Sentinel-2 spectral layers, the six different VIs, the image objects, the S1 VV + VH data sets were normalized to a range of 0–255 (8-bit range) using a linear transformation function. The normalized datasets were stacked into a three different single multi-band image dataset

**Table 3**

Description of data combination scenarios for experimenting the segregation of agroforestry cocoa from open canopy forest and other land cover classes.

Datasets	Description	Number of bands
D1	S2 spectral bands (2,3,4,5,6,7,8) + Six VIs	13
D2	S2 spectral bands (2,3,4,5,6,7,8) + Six VIs + 2 S1 VV, VH bands	15
D3	S2 spectral bands (2,3,4,5,6,7,8) + Six VIs + 2 S1 VV, VH bands + Image objects	16

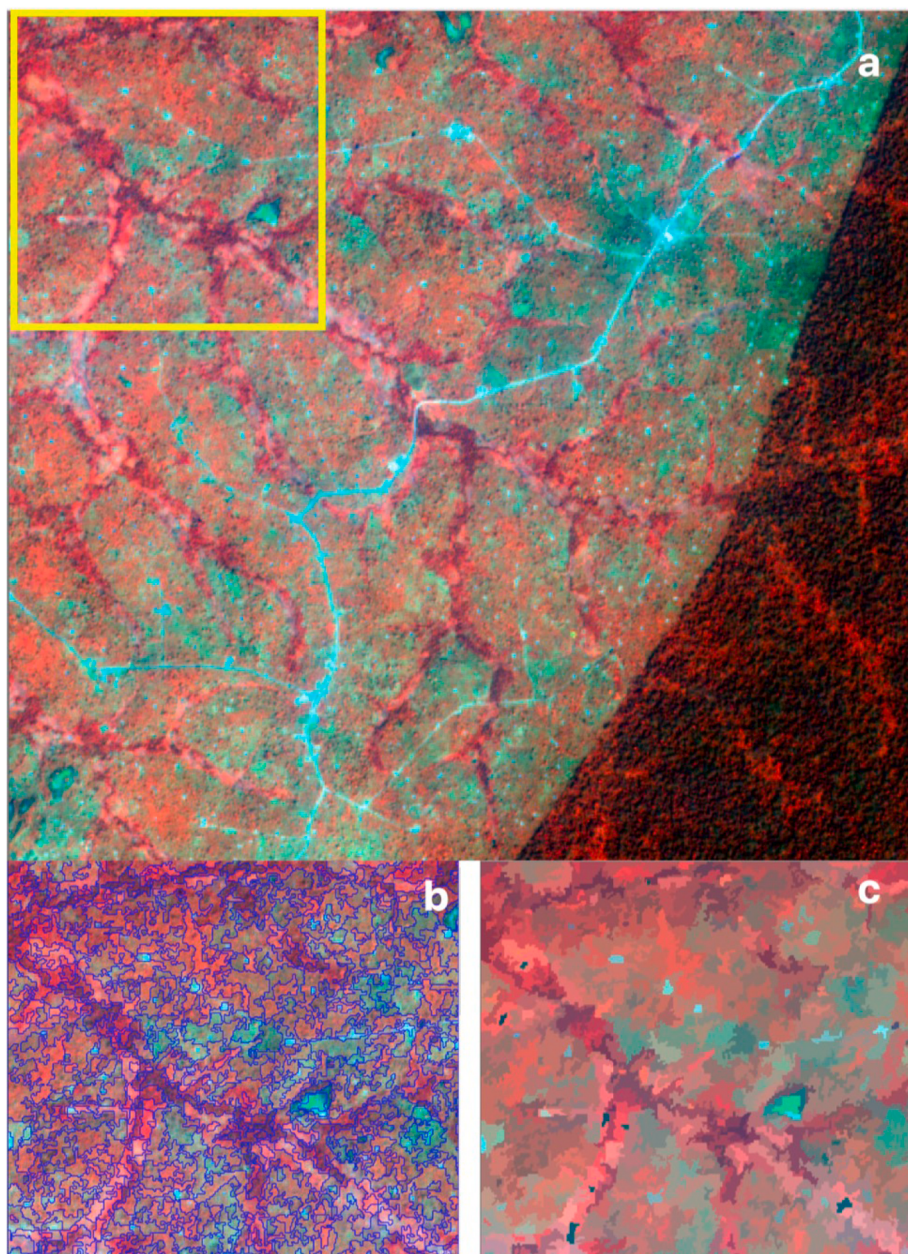


**Fig. 2.** (a) Pixel view of a subset of the Sentinel-2 Image (false colour composite) of the study area used for the visualisation and experimenting the iterative procedure of image segmentation in the eCognition software. (b) Results of segmentation overlayed on pixel based raster image (c) Results of segmentation displayed as object raster. (For interpretation of the references to colour in this figure legend, the reader is referred to the Web version of this article.)

denoted with D (See Table 3). The choice of classification method affects the results of land use/cover mapping (Heydari and Mountrakis, 2018). A plethora of literature has been inconclusive on the best classification method for LULC mapping (Heumann, 2011). A number of classification methods e.g. Maximum Likelihood, Artificial Neural Networks (ANN), Support Vector Machines (SVM), and Random Forest (RF). exist for LULC mapping (Akar and Güngör, 2012; Thanh Noi and Kappas, 2017). Machine learning classifiers e.g. SVM, RF and ANN have been found and widely accepted in literature to produce high classification accuracies and to obtain more reliable information from satellite images in comparison to the traditional parametric classifiers e.g. maximum likelihood (Akar and Güngör, 2012; Maxwell et al., 2018). The Random Forest classification algorithm was selected for this study because it was found to perform better in related research where S1 and S2 were combined for improved land cover mapping (e.g., Gómez, 2017; Lopes et al., 2020; Mercier et al., 2019; Tavares et al., 2019).

The RF classification was performed using the ‘randomForest’ package in R software (e.g., Aguilar et al., 2015; Archer and Kimes, 2008). There are two parameters needed during the model training i.e. the number of predictors taken into consideration at each fork of the tree (*mtry*) and the number of random trees assembled during model building (*ntree*) (Wang et al., 2018). For *ntree*, 500 random trees were used to create the model. This is because values greater than 500 have been shown to have little impact on the overall classification results (Duro et al., 2012; Wang et al., 2018). Also, *mtry* was set to an approximate value of four (4) for all the three data combination scenarios, since the square root of number of overall variable (image bands) gives in general near optimum results (Akar and Güngör, 2012).

The mean decrease accuracy and mean decrease gini available in the R-package were used to assess and rank variables importance (Han et al., 2016; Calle and Urrea, 2011). The mean decrease gini is the ratio of the sums all decreases in gini impurity with respect to a given variable, to

the number of trees (Calle and Urrea, 2011). The mean decrease accuracy quantifies the importance of a variable by measuring the change in prediction accuracy, when the values of the variable are randomly permuted compared to the original observations. The larger the mean decrease gini value, the more important the variable (Han et al., 2016). The 'varImpPlot' function available in the 'randomForest' package was used to plot the mean decrease accuracy and the mean decrease gini graph.

## 2.5. Accuracy assessment and analysis of classification output

The accuracy of the classification output was assessed by generating a confusion matrix. To generate the confusion matrix, the 615 validation points (observed class) were overlayed on the final classified image and the observed class points compared to the coinciding classified pixel. The number of classified pixels that agreed with the reference points; the number of pixels classified as X when it was observed to not be X; the number of pixels not classified as X when it was observed to be X; and number of pixels not classified as X when it was not observed as X, were recorded and presented as a matrix with the observed class as columns

and the classified pixels as rows. Kappa coefficient of agreement, overall, users and producer's accuracies were calculated from the confusion matrix. McNemar's test, a non-parametric based test, was used to assess the statistical significance of differences between the use of S2 spectral bands and derivatives (denoted as D1); the stacked S2 spectral bands and S1 backscatter bands and derivatives (denoted as D2); and the combined S1 and S2 bands and derivatives and the image objects derived from the segmentation process (Mercier et al., 2019; Wang et al., 2018). The McNemar's test was performed using the 'mcnemar.test' in R Software.

## 3. Results

The use of S2 bands and derivatives recorded as overall accuracy (OA) of 79.02% and a kappa (k) of 0.748 (Table 4). Despite the high classification accuracy of 79.02%, there was some confusion between agroforestry cocoa and the open canopy forest class. Out of the ninety (90) reference GPS points for AFC, twenty-three (25.55%) were OCF and twelve (13.33%) MCC. Similarly, out of the hundred (100) reference GPS points for OCF, 19% were classified as AFC. Hence, a producer

**Table 4**  
Error matrix and accuracy report for the three datasets experiment between (D1, D2 and D3).

LULC	Agroforestry cocoa	Croplands/ Shrublands	Built-up/ bare soil	Monoculture cocoa	Closed canopy forest	Open canopy forest	Other tree crops	k	PA	UA
<b>D1- S2 spectral bands (2,3,4,5,6,7,8) + Six VIs</b>										
Agroforestry cocoa	49	0	0	3	4	19	4	0.513	62.03%	54.44%
Croplands/ Shrublands	0	61	5	3	0	0	0	0.862	88.41%	87.14%
Built-up/bare soil	0	2	74	0	0	0	0	0.941	97.37%	92.50%
Monoculture cocoa	12	7	1	53	1	3	2	0.701	67.09%	81.54%
Closed canopy forest	0	0	0	0	154	10	2	0.885	92.77%	90.59%
Open canopy forest	23	0	0	4	9	66	3	0.573	62.86%	66.00%
Other tree crops	6	0	0	2	2	2	29	0.696	70.73%	72.50%
Reference Total	90	70	80	65	170	100	40			
Overall Accuracy									79.02%	
Overall Kappa									0.748	
<b>D2 - S2 spectral bands (2,3,4,5,6,7,8) + Six VIs + 2 S1 VV, VH bands</b>										
Agroforestry cocoa	41	0	0	3	1	19	2	0.459	62.12%	45.56%
Croplands/ Shrublands	1	59	1	3	0	0	0	0.866	92.19%	84.29%
Built-up/bare soil	0	2	79	0	0	0	0	0.979	97.53%	98.75%
Monoculture cocoa	16	8	0	53	1	3	1	0.684	64.63%	81.54%
Closed canopy forest	3	0	0	0	165	10	1	0.924	92.18%	97.06%
Open canopy forest	25	0	0	4	3	66	4	0.585	64.71%	66.00%
Other tree crops	4	1	0	2	0	2	32	0.775	78.05%	80.00%
Reference Total	90	70	80	65	170	100	40			
Overall Accuracy									80.49%	
Overall Kappa									0.765	
<b>D3 - S2 spectral bands (2,3,4,5,6,7,8) + Six VIs + 2 S1 VV, VH bands + Image objects brightness</b>										
Agroforestry cocoa	71	0	0	3	1	11	2	0.764	80.68%	78.89%
Croplands/ Shrublands	0	65	2	3	0	0	0	0.919	92.86%	92.86%
Built-up/bare soil	0	1	78	0	0	0	0	0.978	98.73%	97.50%
Monoculture cocoa	7	4	0	55	0	0	2	0.806	80.88%	84.62%
Closed canopy forest	0	0	0	0	166	5	0	0.963	97.08%	97.65%
Open canopy forest	12	0	0	2	2	84	3	0.794	81.55%	84.00%
Other tree crops	0	0	0	2	1	0	33	0.86	91.67%	82.50%
Reference Total	90	70	80	65	170	100	40			
Overall Accuracy									89.76%	
Overall Kappa									0.877	

accuracy (PA) of 62.03% and a user accuracy (UA) of 54.44%, were recorded for the AFC class. The OCF class recorded a PA of 62.86% and a UA of 66%. The PA of the MCC class was 67.09%. Other tree crops class also recorded a PA of 70.73% and a UA of 72.5%. All the other LULC classes recorded PA and UA above 80%.

The use of the S1 backscatter and S2 spectral bands and derivatives (D2) resulted in an OA of 80.49% and a k of 0.765 (Table 4). Similar to D1, some levels of confusion still remained between the AFC class and the OCF class. Twenty-five (representing 27.77%) of the ninety AFC reference classes were actually OCF classes. A PA of 62.03% was recorded for the AFC class similar to D1, however, the PA declined to 54.44%. Similar results were observed for the OCF class where PA increased slightly to 64.71% and UA 66% remained unchanged compared to results from D1. PA for MCC also declined slightly to 64.63%. PA and UA for Other tree crop class increased to 78.05% and 80%, respectively. Some increase in UA and PA was also observed for the CCF class and the Other tree crops class. The UA of the CCF class increased to 97.06%. Also, PA and UA for Other tree crops class increased to 78.05% and 80%, from 70.73% to 72.50%, respectively.

The final dataset (D3) i.e. the stack of S2 bands and derivatives, S1 backscatter and the Image objects resulted in an increased OA of 89.76% and k of 0.877. Some level of improvement was observed in the segregation of AFC class from OCF classes. The misclassification error decreased from 27.77% to 13.33% for the AFC reference classes captured as OCF. Also, out of the 100 reference dataset for the OFC class, only 11% represented AFC. The PA and UA for the agroforestry cocoa class increased substantially to 80.68% and 78.89% respectively. Equally, the agricultural lands, built-up, monoculture cocoa, closed canopy forest, open canopy forest, and other tree crops obtained PA and UA above 80%.

The variables' importance is based on mean decrease in accuracy and mean decrease in gini score (Fig. 3). Image objects is the most important predictor variable based on the mean decrease in accuracy and the mean decrease in gini scores, indicating the importance of image objects in mapping the landscape. Sentinel-2 red edge 1 and red edge 2 spectral bands were also in the topmost important predictor variables in both scores. Out of six vegetation indices bands, the red-edge chlorophyll index (CI) band ratios was among the most important variables in the random forest classification process. The Sentinel-1 VH and VV bands were the fifth and sixth most important predictor variable based on mean decrease in accuracy, however, the least most important variables based on mean decrease in gini score. This indicates their importance permuting with other variables, though their inclusion did not

significantly affect the overall classification accuracy. McNemar's test of statistical significance between the three datasets experiment between D1 and D3 indicates statistically significant difference (*x-value*: 5.56 and *p-value*: 0.018) as well as the differences between D2 and D3 (*x-value*: 5.50 and *p-value*: 0.019). However, the values for D1 and D2 were not statistically distinct (*x-value*: 1.17 and *p-value*: 0.280).

The final LULC map of the landscape produced using D3, showing cocoa systems (AFC and MCC) clearly isolated from forest cover (CCF and OCF) and other land cover classes (croplands and built-up/bare) are shown in Fig. 4. Table 5 presents the quantitative results of the area of the various LULC classes in the study landscape. Monoculture cocoa and agroforestry dominated the landscape with extents of 1212.37 km<sup>2</sup> (29.75%) and 1047.74 km<sup>2</sup> (25.71%), respectively (Table 5). The monoculture and agroforestry cocoa class occurred in the entire off-reserve landscape. Patches of monoculture and agroforestry cocoa are also observed in the boundaries of the forest reserves, mainly the Krokkosua Hill forest reserve (Fig. 4), an evidence of cocoa extension into forest reserves. The closed canopy forest class, as seen from Fig. 4, is mainly found in the forest reserves and the protected area. The open canopy forest, which constitutes 11.02% of the study landscape, is also observed mainly in the forest reserves and protected area, with patches seen in the off-reserve areas usually along the riparian buffer forming the riparian forest in the landscape. The agricultural lands occur at the peripheries of the built-up areas and also along the road networks in the landscape and occupy 290.91 km<sup>2</sup> (representing 7.14%) of the study area.

Fig. 5 shows a visual comparison of the classification results of D2 and D3. Fig. 5 (a), 5 (c) and 5 (e) shows classification results of D2 and Fig. 5 (b), 5 (d) and 5 (f) shows classification results of D3. A visual inspection of the results from D2 shows a salt-and-pepper or speckles. Comparatively, the visual inspection of the results from D3 shows a more refined classification output with road networks clearly and accurately delineated. In Fig. 5 (c) and (d), an agroforestry cocoa farm blocked during the field validation was better represented using dataset D3 as shown in Fig. 5 (d) compared to D2 as shown in Fig. 5 (c).

#### 4. Discussion

The use of only Sentinel 2 spectral bands and VIs (D1) was unable to segregate between the agroforestry cocoa and open canopy forest, despite a high overall accuracy and kappa coefficient of 79.02% and 0.748, respectively. The classification results using D1 are comparable to those presented in previous studies by Benefoh et al. (2018) where

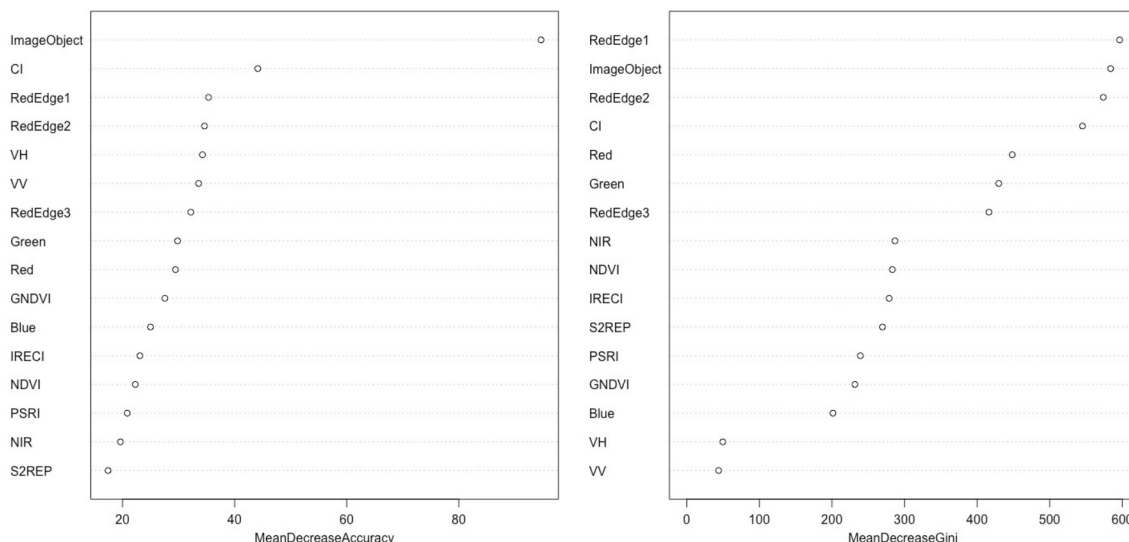
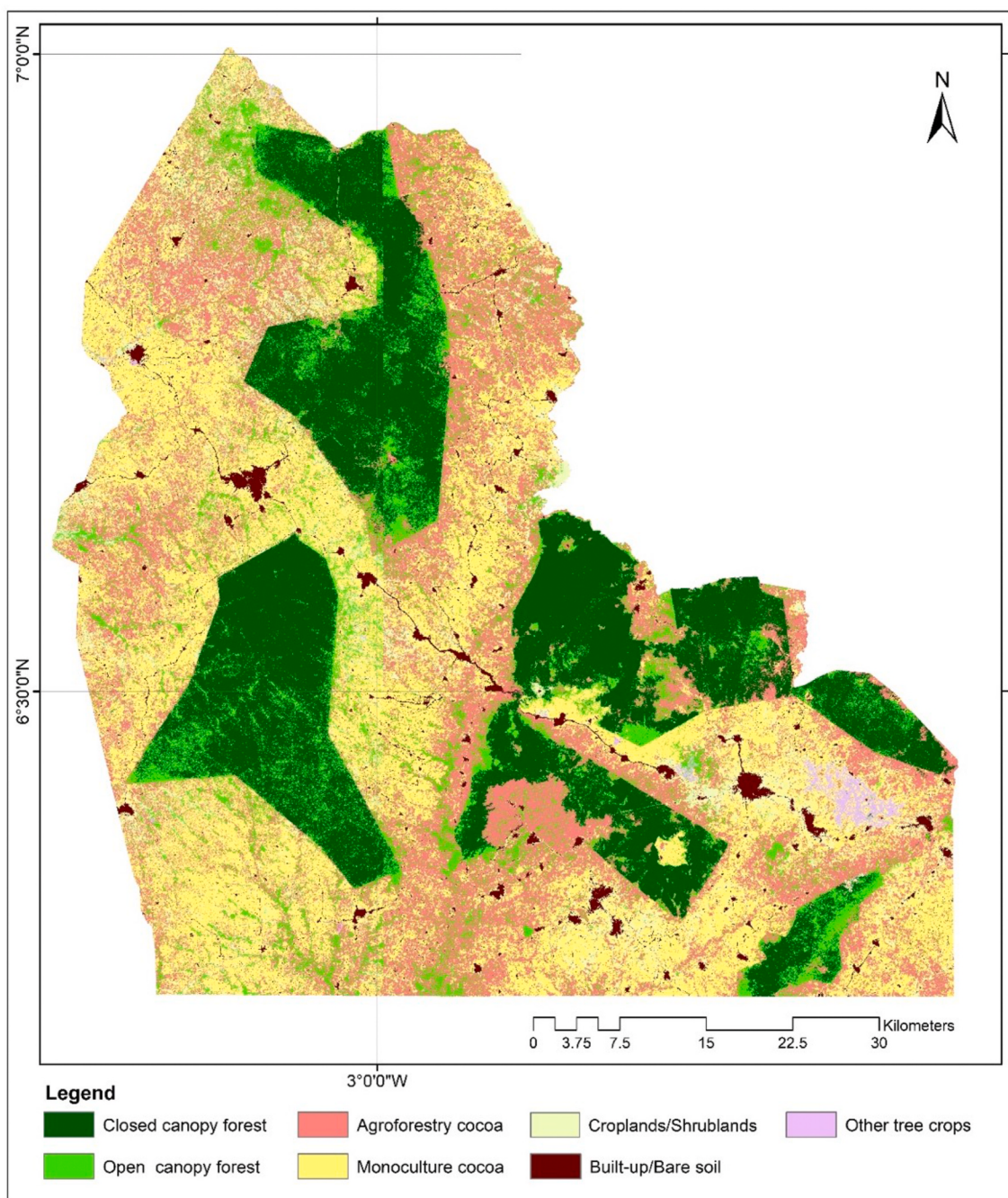


Fig. 3. Variables' importance based on mean decrease in accuracy (left) and mean decrease in gini score (right).



**Fig. 4.** Land use/land cover map of Juaboso-Bia landscape showing the different cocoa systems (monoculture cocoa and agroforestry cocoa) segregated from closed canopy forest and open canopy forest classes to 89.7% overall accuracy.

**Table 5**  
Area (km<sup>2</sup>) of the various LULC classes in the Juaboso-Bia landscape.

LULC Class	Area/km <sup>2</sup>	Percentage
Closed canopy forest	963.79	23.65%
Open canopy forest	449.29	11.02%
Monoculture cocoa	1212.37	29.75%
Agroforestry cocoa	1047.74	25.71%
Croplands/Shrublands	290.91	7.14%
Other tree crops	18.25	0.45%
Built-up/bare soil	92.85	2.28%
<b>Total</b>	<b>4075.18</b>	

optical Landsat 8 images and image fusion approach were used to segregate agroforestry cocoa from open canopy forest, and recorded an overall accuracy of 82.6% and a kappa of 0.73. The confusion matrix, however, revealed some confusion in segregating agroforestry cocoa from monoculture cocoa, open canopy forest and other tree crops. The difficulty in the use of only spectral information to segregate cocoa systems from the forest system can be attributed to spectral similarities between open canopy forest class and the agroforestry cocoa class. Usually, agroforest cocoa plantation has a multi-strata canopy structure, which creates spectral information similar to that of open canopy forest classes. Also, the landscape as described is highly heterogeneous with various levels of patchiness. Theoretically, the pixel value of satellite imagery represents the average value of a measured physical variable, i.e., the total radiance value in a given wavelength band for the specific

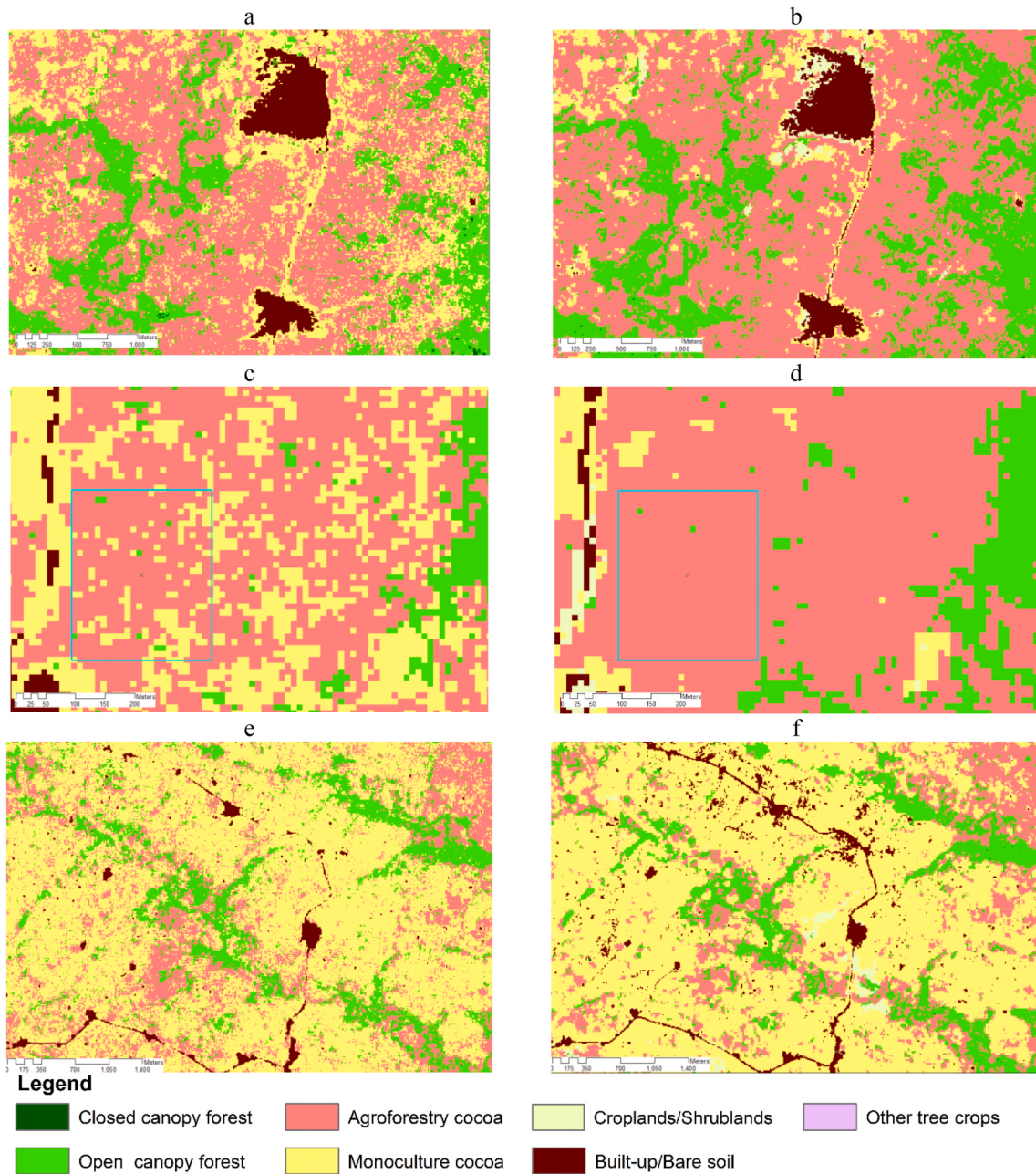


**Fig. 5.** Visual Comparison of classification results of D2 and D3. (a), (c) and (e) shows classification results of D2 and (b), (d) and (f) shows classification results of D3.

ground area covered by pixel. This means that using the S2 spectral datasets and derivatives, the image pixel is the basic processing unit and does not take into consideration the characteristics of the neighboring pixels. The spectral pixels are not a true representation of geographical objects and land use classes in the highly heterogeneous landscape where there is a high degree of pixel variability within a given class; this confuses traditional classifiers resulting in misclassification errors (Salah, 2014; Shackelford and Davis, 2003). This is likely to have resulted in a low Producer and User accuracies in the classification output when S2 spectral bands and derivatives were used.

Adding the SAR S1 dataset and derivatives to the S2 datasets and derivative did not improve significantly the overall accuracy of the classification outcome ( $x$ -value: 1.17 and  $p$ -value: 0.280). This is evident from the mean decreasing Gini graph (in Fig. 3), where SAR S1 VH and VV bands were the least important variables in the Random Forest classification. This finding is corroborated by Mercier et al. (2019) in a

similar effort to map a forest–agriculture mosaics in a heterogeneous landscape using SAR S-1 and optical S-2. They observed that, the C-band SAR S1 data was not relevant in the classification of the various vegetation classes. Also, C band SAR is less suitable for forest mapping due to low penetration depth and rapid signal saturation (Mercier et al., 2019; Woodhouse, 2017). On the contrary, Gómez (2017) and Lopes et al. (2020) reported improved classification accuracy for combined use of S1 and S2 for land cover mapping of an agricultural landscape. Notwithstanding, slight increment were observed in overall accuracy (from 79.02% to 80.49%) and kappa (from 0.748 to 0.765). However, the difficulty of segregating agroforestry cocoa from open canopy forest still remained. This may be because SAR sensors are sensitive to vegetation structure and agroforestry cocoa and open canopy forest classes are characterized by their structural similarities i.e multi-strata canopy structure with low canopy closure. This structural similarity implies difficulties in segregating them using SAR S1 dataset.

Despite the lack of statistically significant contribution of the S1 dataset to the overall classification accuracy of the landscape, class level improvement in producer and user accuracy was observed for the closed canopy forest class, other tree crops class and the built-up class. The closed canopy forest class and other tree crops (*Citrus*, *Rubber* etc.) are characterized by uniform canopy structure and usually appear in large dense patches. S1 dataset is sensitive to dense and uniform canopy structure and hence scattered by the upper canopy (Woodhouse, 2017), therefore providing additional structural information which improved the separability of the closed canopy forest class and other tree crops, hence the improved producer and user accuracy. However, producer accuracy for monoculture cocoa declined from 67.09% to 64.63%. The decline was as a result of misclassification of some agroforestry cocoa as monoculture cocoa (Table 4).

The final dataset, i.e. the combined use of image spectral and backscatter bands and image objects significantly improved the overall classification output. An overall classification accuracy and kappa of 89.76% and 0.877 respectively were obtained. Chen et al. (2018); Salah (2014); and Salehi et al. (2013, 2011) similarly reported higher classification accuracies when image objects were combined with spectral pixels for land cover mapping. The sole use of the rich spectral information contained in the 10 m spatial resolution S2 dataset implies there is spectral high variability within the agroforestry cocoa class and open canopy forest cover class coupled with the inherent speckles associated with the radar S1 datasets. By the definition of agroforestry cocoa (see Table 1), a 1-acre (4046 sq m) agroforestry cocoa farm is likely to be represented by an average of 40 Sentinel-2 pixels with high probability of spectral variations between the 40 pixels which may consequently result in misclassification errors leading to low PA and UA. On the other hand, the image objects provide a generalization of the spectral information defined by the segmentation criteria. This generalization aggregates spectral variation within classes and amplifies the distinction between classes, therefore improves the efficiency of classification (Wang et al., 2004). Combining image objects with spectral pixels implies that the classification method does not operate directly on single pixels only but also on several pixels that have been clustered into a single meaningful object through the process of image segmentation (Shackelford and Davis, 2003). As depicted (Fig. 2), the use of optical and radar bands (D2) despite the high accuracy (OA = 80.49%, k = 0.765) resulted in a salt-and-pepper effect due to high levels of spectral heterogeneity within a class patch and also due to speckles associated with radar datasets. Compared to the combined use of spectral, backscatter and image objects (D3) which yielded a more refined classification output with higher class level user reliability (OA = 89.49%, k = 0.877). For example, PA and UA of 80.68% and 78.89%, respectively, were obtained for the agroforest cocoa class using the combined approach as compared to a PA of 62.12% and a UA of 45.56% using the spectral and backscatter bands (Table 4). An additional image filtering process could be applied to reduce the salt-and-pepper effect, but this implies losing specific details such as road networks, drainage channels and compromises the overall spatial resolution of the dataset. This will subsequently affect the overall accuracy of the classification output, hence the right choice of using image objects through segmentation process.

## 5. Conclusions

In this research, several spectral, textural, and morphological variables were extracted from optical Sentinel-2 and radar C Band Sentinel-1, and then subjected to Random Forest machine learning classification procedure to produce a LULC map of the cocoa-forest mosaic landscape of Ghana. Sentinel-2 spectral bands, Sentinel-1 radar VV and VH backscatter bands, and image objects derived from segmentation are beneficial in providing sustainable, relatively accurate representation of land use classes and cost-effective approaches to mapping Ghana's cocoa-forest mosaic landscape to a high classification accuracy. Combining

spectral pixels with image objects derived from image segmentation significantly increases overall classification accuracy and specifically, the accuracy of isolating agroforestry cocoa systems from forest cover and other land cover classes in the cocoa-forest mosaic landscape of Ghana. This classification approach is suitable for highly heterogeneous landscapes such as the cocoa-forest mosaic landscape of Ghana, where within class spectral variability is high and class definitions are based on spatial configuration or morphology of the class.

It is however worth noting that, image objects created from the image segmentation process depends on the segmentation scale, the spatial resolution of the dataset used, and class definitions etc. Therefore, different datasets and mapping extent or scale will require different levels of image objects. Once an object is wrongly delineated or assigned, all pixels in the object will be misclassified, which will affect the general classification performance. Future research is therefore recommended to emphasise on different segmentation parameters to determine the optimum thresholds. Also, more robust algorithms should be experimented for different image datasets, different mapping scale and different landscape conditions within the cocoa-forest mosaic landscape with the ultimate aim of improving the segregation of agroforestry cocoa from open canopy forest class and other land cover classes.

The final LULC map produced provides a real context to the cocoa monoculture and agroforestry cocoa coverage discourse. It provides critical applications under the Cocoa and Forests Initiative, to support government-led monitoring and the private sector's commitment to halt cocoa-driven deforestation. Furthermore, and most importantly, the map shows agroforestry cocoa from monoculture cocoa, which provides a tremendous boost to monitoring landscape-level improvements associated with the promotion and adoption of agroforestry as a climate-smart practice and also for monitoring various off-reserve landscape forest restoration activities. This research holds applications for government-led monitoring and the private sector's commitment to halt cocoa-driven deforestation. It also feeds into improvements in national forest monitoring framework for REDD+ accounting as well as private sector and national commitments towards deforestation-free cocoa supply chains in Ghana and the West African cocoa belt.

## Ethical statement

The authors declare that all ethical practices have been followed in relation to the development, writing, and publication of the article.

## CRediT authorship contribution statement

**George Ashiagbor:** Conceptualization, Investigation, Methodology, Formal analysis, Writing - original draft, Writing - review & editing. **Eric K. Forkuo:** Writing - review & editing, Validation, Supervision. **Winston A. Asante:** Conceptualization, Investigation, Writing - review & editing, Supervision. **Emmanuel Acheampong:** Conceptualization, Writing - review & editing. **Jonathan A. Quaye-Ballard:** Writing - review & editing, Validation, Supervision. **Prince Boamah:** Resources, Methodology. **Yakubu Mohammed:** Resources, Methodology. **Ernest Foli:** Writing - review & editing.

## Declaration of competing interest

The authors declare that they have no known competing financial interests or personal relationships that could have appeared to influence the work reported in this paper.

## Acknowledgements

This study was funded by the UK Space Agency as part of the International Partnerships Programme through Ecometrica under the Forests 2020 Project. The authors appreciate the inputs of the Forests 2020 team

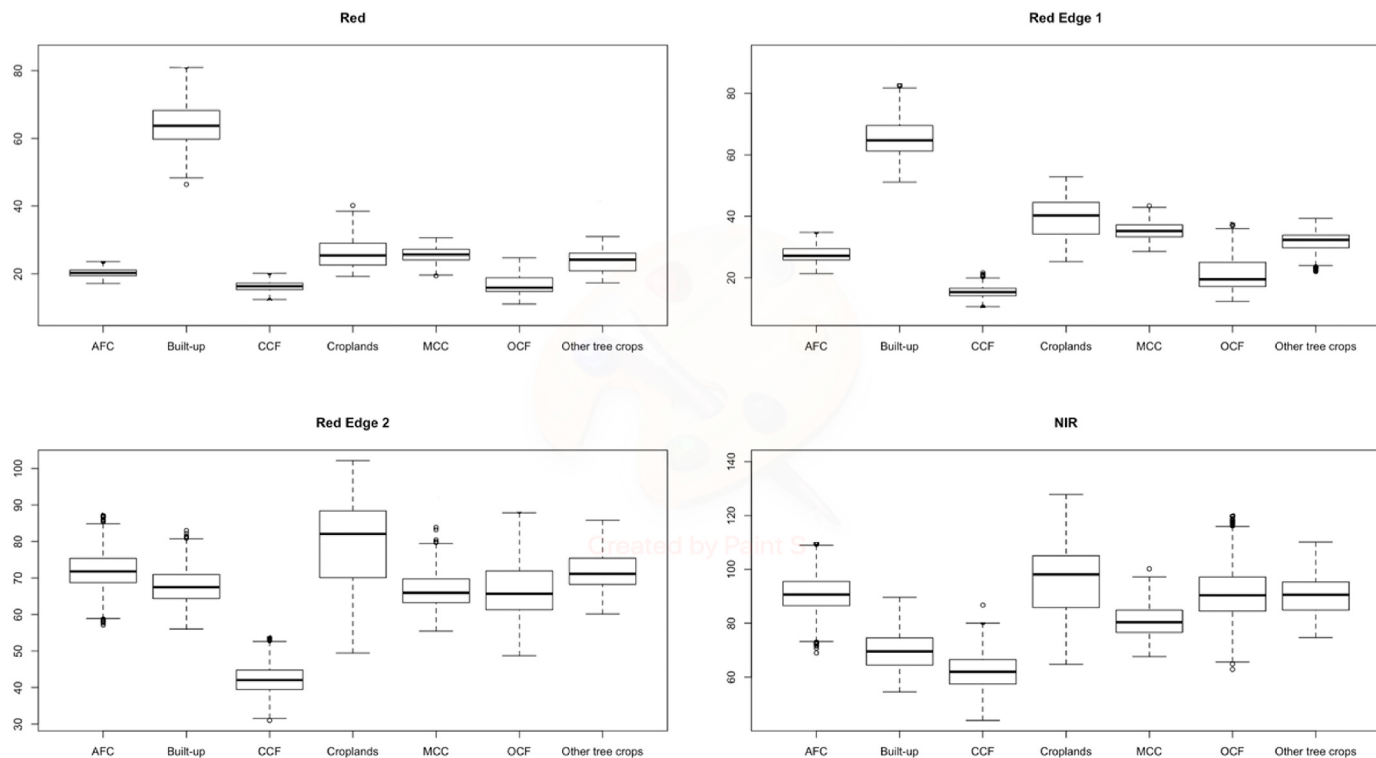
members at Ecometrica, particular, Ruth Malleson, Sarah Middlemiss and Richard Tipper for the institutional support under the Forests 2020 collaboration. We are also grateful to the Forest 2020 team at the University of Leicester, particularly, Yaqing Gou for providing technical

support in data processing. Also to the many administrative and field staff at the Resource Management Support Centre (RMSC), Forestry Commission of Ghana and the Kwame Nkrumah University of Science and Technology for supporting this study at various stages.

## Appendix A. Supplementary data

Supplementary data to this article can be found online at <https://doi.org/10.1016/j.rsase.2020.100349>.

### Appendix 1 Box plot showing spectral overlap between vegetation classes in four Sentinel-2 spectral bands



## References

- Aguilar, M., Vallario, A., Aguilar, F., Lorca, A., Parente, C., 2015. Object-based greenhouse horticultural crop identification from multi-temporal satellite imagery: a case study in almeria, Spain. *Rem. Sens.* 7, 7378–7401. <https://doi.org/10.3390/rs70607378>.
- Akar, Ö., Güngör, O., 2012. Classification of multispectral images using Random Forest algorithm. *J. Geod. Geoinf.* 1, 105–112. <https://doi.org/10.9733/jgg.241212.1>.
- Akinyemi, Felicia, 2013. An assessment of land-use change in the Cocoa Belt of southwest Nigeria. *Int. J. Rem. Sens.* 34 (8), 2858–2875. <https://doi.org/10.1080/0143161.2012.753167>. In this issue.
- Anane, F., Padi, F., 2016. Baseline farmer survey of smallholder cocoa farming systems in Ghana. *Sustain. Agric. Res.* 6 (1), 13. <https://doi.org/10.5539/sar.v6n1p13>.
- Archer, K.J., Kimes, R.V., 2008. Empirical characterization of random forest variable importance measures. *Comput. Stat. Data Anal.* 52, 2249–2260. <https://doi.org/10.1016/j.csda.2007.08.015>.
- Asante, W., Dawoe, E.L.K., Acheampong, E., Bosu, P.P., 2017. A new perspective on forest definition and shade regimes for Redd+ interventions in Ghana's cocoa landscape. *Ghana J. For.* 33, 1–15. <https://doi.org/10.13140/RG.2.2.14758.42564>.
- Balzter, H., Cole, B., Thiel, C., Schmullius, C., 2015. Mapping CORINE land cover from Sentinel-1A SAR and SRTM digital elevation model data using random forests. *Rem. Sens.* 7, 14876–14898. <https://doi.org/10.3390/rs71114876>.
- Ban, Y., Webber, L., Gamba, P., Paganini, M., 2017. EO4Urban: sentinel-1A SAR and Sentinel-2A MSI data for global urban services. In: 2017 Jt. Urban Remote Sens. Event. <https://doi.org/10.1109/JURSE.2017.7924550>. JURSE 2017 0–3.
- Barati, S., Rayegani, B., Saati, M., Sharifi, A., Nasri, M., 2011. Comparison the accuracies of different spectral indices for estimation of vegetation cover fraction in sparse vegetated areas. *Egypt. J. Remote Sens. Sp. Sci.* 14, 49–56. <https://doi.org/10.1016/j.ejrs.2011.06.001>.
- Barima, Yao Sadaiou Sabas, Kouakou, Akoua Tamia Madeleine, Bamba, Issouf, Sangne, Yao Charles, Godron, Michel, Andrieu, Julien, Bogaert, Jan, 2016. Cocoa crops are destroying the forest reserves of the classified forest of Haut-Sassandra (Ivory Coast). *Global Ecol. Conserv.* 8, 85–98. <https://doi.org/10.1016/j.gecco.2016.08.009>.
- Basayigit, L., Ersan, R., 2015. Comparison of Pixel-Based and Object-Based Classification. *Bayanudin, A.A., Jatmiko, R.H., 2016. Orthorectification of sentinel-1 SAR (synthetic aperture radar) data in some parts of south-eastern sulawesi using sentinel-1 toolbox. In: IOP Conference Series: Earth and Environmental Science.* <https://doi.org/10.1088/1755-1315/47/1/012007>.
- Benefoh, D.T., 2018. Assessing Land-Use Dynamics in a Ghanaian Cocoa Landscape. *Benefoh, D.T., Villamor, G.B., Noordwijk, M. Van, Borgemeister, C., Asante, W.A., Asubonteng, K.O., 2018. Assessing land-use typologies and change intensities in a structurally complex Ghanaian cocoa landscape. Appl. Geogr.* 99, 109–119. <https://doi.org/10.1016/j.apgeog.2018.07.027>.
- Birth, G.S., McVey, G.R., 1968. Measuring the color of growing turf with a reflectance spectrophotometer 1. *Agron. J.* 60 (6), 640–643. <https://doi.org/10.2134/agronj1968.00021962006000060016x>.
- Blaschke, T., Strobl, J., 2001. What's wrong with pixels? Some recent developments interfacing remote sensing and GIS. *Zeitschrift für Geoinformationssysteme* 12–17.
- Blaser, W.J., Oppong, J., Hart, S.P., Landolt, J., Yeboah, E., Six, J., 2018. Climate-smart sustainable agriculture in low-to-intermediate shade agroforests. *Nature Sustainability* 1 (5), 234–239. <https://doi.org/10.1038/s41893-018-0062-8>.
- Calle, M.L., Urrea, V., 2011. Letter to the editor: stability of random forest importance measures. *Briefings Bioinf.* 12 (1), 86–89. <https://doi.org/10.1093/bib/bbq011>.

- Carodenuto, S., 2019. Governance of zero deforestation cocoa in West Africa: new forms of public–private interaction. *Environ. Policy Gov.* 29, 55–66. <https://doi.org/10.1002/eet.1841>.
- Chatziantoniou, A., Petropoulos, G.P., Psomiadis, E., 2017. Co-Orbital Sentinel 1 and 2 for LULC mapping with emphasis on wetlands in a mediterranean setting based on machine learning. *Rem. Sens.* 9 <https://doi.org/10.3390/rs9121259>.
- Chen, Yuehong, Zhou, Y., Ge, Y., An, R., Chen, Yu, 2018. Enhancing land cover mapping through integration of pixel-based and object-based classifications from remotely sensed imagery. *Rem. Sens.* 10 <https://doi.org/10.3390/rs10010077>.
- Choi, H., Jeong, J., 2019. Speckle noise reduction technique for SAR images using statistical characteristics of speckle noise and discrete wavelet transform. *Rem. Sens.* 11 (10), 1184. <https://doi.org/10.3390/rs11101184>.
- Clerici, N., Valbuena Calderón, C.A., Posada, J.M., 2017. Fusion of Sentinel-1A and Sentinel-2A data for land cover mapping: a case study in the lower Magdalena region, Colombia. *J. Maps* 13, 718–726. <https://doi.org/10.1080/17445647.2017.1372316>.
- Cutler, M.E.J., Boyd, D.S., Foody, G.M., Vettrivel, A., 2012. ISPRS Journal of Photogrammetry and Remote Sensing Estimating tropical forest biomass with a combination of SAR image texture and Landsat TM data : an assessment of predictions between regions. *ISPRS J. Photogrammetry Remote Sens.* 70, 66–77. <https://doi.org/10.1016/j.isprsjprs.2012.03.011>.
- Delegido, J., Verrelst, J., Alonso, L., Moreno, J., 2011. Evaluation of sentinel-2 red-edge bands for empirical estimation of green LAI and chlorophyll content. *Sensors* 11, 7063–7081. <https://doi.org/10.3390/si110707063>.
- Drăguț, L., Tiede, D., Levick, S.R., 2010. ESP: a tool to estimate scale parameter for multiresolution image segmentation of remotely sensed data. *Int. J. Geogr. Inf. Sci.* 24, 859–871. <https://doi.org/10.1080/13658810903174803>.
- Duro, D.C., Franklin, S.E., Dubé, M.G., 2012. Remote Sensing of Environment A comparison of pixel-based and object-based image analysis with selected machine learning algorithms for the classification of agricultural landscapes using SPOT-5 HRG imagery. *Remote Sens. Environ.* 118, 259–272. <https://doi.org/10.1016/j.rse.2011.11.020>.
- El-shehaby, A., Taha, L.G.E., 2018. A novel classifier ensemble for combining pixel-based and object based classification methods for improving feature extraction from LIDAR intensity data and LIDAR derived layers. *Am. J. Geogr. Inf. Syst.* 7, 75–81. <https://doi.org/10.5923/j.agjis.20180703.01>.
- ESA, 2012. ESA's Radar Observatory Mission for GMES Operational Services. ESA Special Publication. <https://doi.org/10.1016/j.jrse.2011.11.026>.
- ESA, 2015. ESA's Optical High-Resolution Mission for GMES Operational Services. Forestry Commission, 2016. Ghana REDD + Strategy.
- Fountain, A., Huetz-Adams, F., 2018. Cocoa Barometer.
- Frampton, W.J., Dash, J., Watmough, G., Milton, E.J., 2013. Evaluating the capabilities of Sentinel-2 for quantitative estimation of biophysical variables in vegetation. *ISPRS J. Photogrammetry Remote Sens.* 82, 83–92. <https://doi.org/10.1016/j.isprsjprs.2013.04.007>.
- Ghassemian, H., 2016. A review of remote sensing image fusion methods. *Inf. Fusion* 32, 75–89. <https://doi.org/10.1016/j.inffus.2016.03.003>.
- Gibbs, H.K., Brown, S., Niles, J.O., Foley, J.A., 2007. Monitoring and estimating tropical forest carbon stocks: making REDD a reality. *Environ. Res. Lett.* 2 <https://doi.org/10.1088/1748-9326/2/4/045023>.
- Gómez, M.G.C., 2017. Joint Use of Sentinel-1 and Sentinel-2 for Land Cover Classification: A Machine Learning Approach 72.
- Hackman, K.O., Gong, P., Wang, J., 2017. New land-cover maps of Ghana for 2015 using Landsat 8 and three popular classifiers for biodiversity assessment. *Int. J. Rem. Sens.* 38, 4008–4021. <https://doi.org/10.1080/01431161.2017.1312619>.
- Han, H., Guo, X., Yu, H., 2016. August. Variable selection using mean decrease accuracy and mean decrease gini based on random forest. In: 2016 7th Ieee International Conference on Software Engineering and Service Science (Icsess). IEEE, pp. 219–224. <https://doi.org/10.1109/ICSESS.2016.7883053>.
- Heumann, B.W., 2011. An object-based classification of mangroves using a hybrid decision tree—support vector machine approach. *Rem. Sens.* 3, 2440–2460. <https://doi.org/10.3390/rs3112440>.
- Heydari, S.S., Mountrakis, G., 2018. Effect of classifier selection, reference sample size, reference class distribution and scene heterogeneity in per-pixel classification accuracy using 26 Landsat sites. *Remote Sens. Environ.* 204, 648–658. <https://doi.org/10.1016/j.rse.2017.09.035>.
- Higonet, E., Bellantonio, M., Hurowitz, G., 2017. Chocolate's Dark Secret; How the Cocoa Industry Destroys National Parks.
- Hoare, A., King, R., Airey, S., 2018. Cocoa trade, climate change and deforestation [WWW Document]. Chatham House. URL [https://resourcetrade.earth/stories/cocoa-trade-climate-change-and-deforestation?\\_ga=2.18191361.707459656.1557546911-2054109385.1557546911&\\_ga=1.258761464.1557546911.1557546911-2054109385.1557546911&\\_ga=1.258761464.1557546911.1557546911-2054109385.1557546911](https://resourcetrade.earth/stories/cocoa-trade-climate-change-and-deforestation?_ga=2.18191361.707459656.1557546911-2054109385.1557546911&_ga=1.258761464.1557546911.1557546911-2054109385.1557546911&_ga=1.258761464.1557546911.1557546911-2054109385.1557546911).
- International Cocoa Initiative (ICI), 2011. Cocoa farming: an overview. [https://cocoainitiative.org/wp-content/uploads/2016/09/ECA\\_-2011\\_-Cocoa\\_Farming\\_an\\_overview.pdf](https://cocoainitiative.org/wp-content/uploads/2016/09/ECA_-2011_-Cocoa_Farming_an_overview.pdf).
- IDH, 2018. Ghana Cocoa & Forests Initiative National Implementation Plan 2018–2020 1–46.
- Indufor, Oy, 2015. Development of Reference Emissions Levels and Measurement, Reporting and Verification System in Ghana (Helsinki).
- Joshi, N., Baumann, M., Ehammer, A., Fensholt, R., Grogan, K., Hostert, P., Jepsen, M.R., Kuemmerle, T., Meyfroidt, P., Mitchard, E.T.A., Reiche, J., Ryan, C.M., Waske, B., 2016. A review of the application of optical and radar remote sensing data fusion to land use mapping and monitoring. *Rem. Sens.* 8, 1–23. <https://doi.org/10.3390/rs8010070>.
- Kaplan, G., Avdan, U., 2018. Sentinel-1 and sentinel-2 data fusion for mapping and monitoring wetlands 1–12. <https://doi.org/10.20944/preprints201807.0244.v1>.
- Kroeger, A., Bakhtary, H., Haupt, F., Streck, C., 2017. Eliminating Deforestation from the Cocoa Supply Chain.
- Li, X., Meng, Q., Gu, X., Jancso, T., Yu, T., Wang, K., 2013. A hybrid method combining pixel-based and object-oriented methods and its application in Hungary using Chinese HJ-1 satellite images. *Int. J. Rem. Sens.* 34, 4655–4668. <https://doi.org/10.1080/01431161.2013.780669>.
- Liu, C., 2016. Analysis of Sentinel-1 SAR Data for Mapping Standing Water in the Twente Region 37.
- Liu, D., Xia, F., 2010. Assessing object-based classification: advantages and limitations. *Remote Sens. Lett.* 1, 187–194. <https://doi.org/10.1080/01431161003743173>.
- Lopes, M., Frison, P., Crowson, M., Warren-Thomas, E., Hariyadi, B., Kartika, W.D., Agus, F., Hamer, K.C., Stringer, L., Hill, J.K., Pettorelli, N., 2020. Improving the accuracy of land cover classification in cloud persistent areas using optical and radar satellite image time series. *Methods Ecol. Evol.* <https://doi.org/10.1111/210X.13359>, 2041–210X.13359.
- Lu, D., Weng, Q., 2007. A survey of image classification methods and techniques for improving classification performance. *Int. J. Rem. Sens.* <https://doi.org/10.1080/01431160600746456>.
- Maghsoodi, Y., Collins, M.J., Leckie, D., 2012. Speckle reduction for the forest mapping analysis of multi-temporal Radarsat-1 images. *Int. J. Rem. Sens.* 33, 1349–1359. <https://doi.org/10.1080/01431161.2011.568530>.
- Mahmood, A.R.J., 2017. Ghana High Forest Zone Forest Change Maps 2000–2015 Accuracy Assessment Report.
- Maxwell, A.E., Warner, T.A., Fang, F., Maxwell, A.E., Warner, T.A., Implementation, F.F., Maxwell, A.E., Warner, T.A., 2018. Implementation of machine-learning classification in remote sensing : an applied review. *Int. J. Rem. Sens.* 39, 2784–2817. <https://doi.org/10.1080/01431161.2018.1433343>.
- Mercier, A., Betbeder, J., Rumiano, F., Baudry, J., Gond, V., Blanc, L., Bourgoin, C., Cornu, G., Ciudad, C., Marchamalo, M., Poccard-Chapuis, R., Hubert-Moy, L., 2019. Evaluation of sentinel-1 and 2 time series for land cover classification of forest-agriculture mosaics in temperate and tropical landscapes. *Rem. Sens.* 11, 979. <https://doi.org/10.3390/rs11080979>.
- Mertens, Benoît, Lambin, Eric F., 2000. Land-cover-change trajectories in Southern Cameroon. *Ann. Assoc. Am. Geogr.* 90 (3), 467–494. <https://doi.org/10.1111/0004-5608.00205>. In this issue.
- Mitchell, A.L., Rosenqvist, A., Mora, B., 2017. Current remote sensing approaches to monitoring forest degradation in support of countries measurement, reporting and verification (MRV) systems for REDD+. *Carbon Bal. Manag.* <https://doi.org/10.1186/s13021-017-0078-9>.
- National REDD+ Secretariat, Forest Commission, 2017. Ghana's National Forest Reference Level.
- Numbisi, F.N., Van Coillie, F.M.B., De Wulf, R., 2019. Delineation of cocoa agroforests using multisession sentinel-1 SAR images: a low grey level range reduces uncertainties in glcm texture-based mapping. *ISPRS Int. J. Geo-Inf.* 8, 179. <https://doi.org/10.3390/ijgi8040179>.
- Odoom, F., Varmola, M., 1998. Hardwood Plantations in Ghana. Forest Plantations Working Papers. Forest Resources Division, FAO, Rome, pp. 1–77. Working Paper FP/24.
- Onojeghuo, A.O., Blackburn, G.A., Wang, Q., Atkinson, P.M., Kindred, D., Miao, Y., 2018. Mapping paddy rice fields by applying machine learning algorithms to multi-temporal Sentinel-1A and Landsat data. *Int. J. Rem. Sens.* 39, 1042–1067. <https://doi.org/10.1080/01431161.2017.1395969>.
- Pasco Corporation, 2013. Mapping of Forest Cover and Carbon Stock in Ghana.
- Pearson, C.A., Covarrubias, J.M., Zissermann, D., Miller, T.G., Gibson, F.P., Haglund, R., Morrison, W., Westley, G., 1972. Spectroscopic factors from the reactions 12C (d, n) 13N and 12C (d, p) 13C using the WBP model. *Nucl. Phys.* 191 (1), 1–18. [https://doi.org/10.1016/0375-9474\(72\)90590-8](https://doi.org/10.1016/0375-9474(72)90590-8).
- Plank, S., Jüssi, M., Martinis, S., Twele, A., Palsar, A., Plank, S., Jüssi, M., Martinis, S., 2017. Mapping of flooded vegetation by means of polarimetric Sentinel-1 and ALOS-2/PALSAR-2 imagery. *Int. J. Rem. Sens.* 38, 3831–3850. <https://doi.org/10.1080/01431161.2017.1306143>.
- Rakatama, A., Pandit, R., Ma, C., Iftekhar, S., 2017. The costs and benefits of REDD+: a review of the literature. *For. Policy Econ.* 75, 103–111. <https://doi.org/10.1016/j.fpol.2016.08.006>.
- Ruf, F.O., 2011. The myth of complex cocoa agroforests: the case of Ghana. *Hum. Ecol.* 39 (3), 373. <https://doi.org/10.1007/s10745-011-9392-0>.
- Salah, M., 2014. Combining pixel-based and object-oriented support vector machines using bayesian probability theory. *ISPRS Ann. Photogramm. Remote Sens. Spat. Inf. Sci.* II-7, 67–74. <https://doi.org/10.5194/isprsaannals-II-7-67-2014>.
- Salehi, B., Zhang, Y., Zhong, M., 2011. Combination of object-based and pixel-based image analysis for classification of vhr imagery over urban areas. In: *Am. Soc. Photogramm. Remote Sens. Annu. Conf.* 2011, pp. 454–460.
- Salehi, B., Zhang, Y., Zhong, M., 2013. A combined object- and pixel-based image analysis framework for urban land cover classification of VHR imagery. *Photogramm. Eng. Rem. Sens.* 79, 999–1014. <https://doi.org/10.14358/PERS.79.11.999>.
- Shackelford, A.K., Davis, C.H., 2003. A combined fuzzy pixel-based and object-based approach for classification of high-resolution multispectral data over urban areas. *IEEE Trans. Geosci. Rem. Sens.* 41, 2354–2363. <https://doi.org/10.1109/TGRS.2003.815972>.
- Somarriba, E., Lopez-Sampson, A., 2018. Coffee and Cocoa Agroforestry Systems : Pathways to Deforestation , Reforestation , and Tree Cover Change.
- Tavares, P.A., Beltrão, N.E.S., Guimarães, U.S., Teodoro, A.C., 2019. Integration of sentinel-1 and sentinel-2 for classification and LULC mapping in the urban area of

- Belém, eastern Brazilian Amazon. Sensors 19. <https://doi.org/10.3390/s19051140>. Switzerland.
- Thanh Noi, P., Kappas, M., 2017. Comparison of random forest, k-nearest neighbor, and support vector machine classifiers for land cover classification using sentinel-2 imagery. Sensors 18, 18. <https://doi.org/10.3390/s18010018>.
- Van Beijma, S., Comber, A., Lamb, A., 2014. Random forest classification of salt marsh vegetation habitats using quad-polarimetric airborne SAR, elevation and optical RS data. Remote Sens. Environ. 149, 118–129. <https://doi.org/10.1016/j.rse.2014.04.010>.
- Wang, L., Sousa, W.P., Gong, P., 2004. Integration of object-based and pixel-based classification for mapping mangroves with IKONOS imagery. Int. J. Rem. Sens. 25, 5655–5668. <https://doi.org/10.1080/01431602331291215>.
- Wang, D., Wan, B., Qiu, P., Su, Y., Guo, Q., Wu, X., 2018. Artificial mangrove species mapping using pléiades-1: an evaluation of pixel-based and object-based classifications with selected machine learning algorithms. Rem. Sens. 10, 294. <https://doi.org/10.3390/rs10020294>.
- WCF, 2019. Action plans to end deforestation. Relied by action plans to end deforestation released by governments of côte d'Ivoire & Ghana and leading chocolate & cocoa companies. <https://www.worldcocoafoundation.org/press-release/action-plans-to-end-deforestation-released-by-governments-of-cote-divoire-and-ghana-and-leading-chocolate-cocoa-companies/>. Accessed: 7th June, 2019.
- Woodhouse, I.H., 2017. Introduction to microwave remote sensing, introduction to microwave remote sensing. <https://doi.org/10.1201/9781315272573>.
- Xie, Y.H., Yue, Y.J., Science, R.S., 2008. Vegetation identification using combined object-oriented and pixel based classification method. In: Proceedings of Information Technology and Environmental System Sciences, pp. 262–268.
- Xiong, J., Thenkabail, P.S., Tilton, J.C., Gumma, M.K., Teluguntla, P., Oliphant, A., Congalton, R.G., Yadav, K., Gorelick, N., 2017. Nominal 30-m cropland extent map of continental Africa by integrating pixel-based and object-based algorithms using Sentinel-2 and Landsat-8 data on google earth engine. Rem. Sens. 9, 1–27. <https://doi.org/10.3390/rs9101065>.
- Yu, Z., Wang, W., Li, C., Liu, W., Yang, J., 2018. Speckle noise suppression in SAR images using a three-step algorithm. Sensors 18 (11), 3643. <https://doi.org/10.3390/s18113643>.
- Zarco-Tejada, P.J., Hornero, A., Hernández-Clemente, R., Beck, P.S.A., 2018. Understanding the temporal dimension of the red-edge spectral region for forest decline detection using high-resolution hyperspectral and Sentinel-2a imagery. ISPRS J. Photogrammetry Remote Sens. 137, 134–148. <https://doi.org/10.1016/j.isprsjprs.2018.01.017>.
- Zhang, Z., Liu, M., Liu, X., Zhou, G., 2018. A new vegetation index based on multitemporal sentinel-2 images for discriminating heavy metal stress levels in rice. Sensors 18. <https://doi.org/10.3390/s18072172>.